

## Supporting Information

for

### **The Protein Corona of PEGylated PGMA-based Nanoparticles is Preferentially Enriched with Specific Serum Proteins of Varied Biological Function**

P.S.R. Naidu<sup>1,2</sup>, M. Norret<sup>1</sup>, N.M. Smith<sup>1,2</sup>, S.A. Dunlop<sup>2</sup>, N.L. Taylor<sup>1,3</sup>, M. Fitzgerald<sup>2,4</sup>  
and K. Swaminathan Iyer<sup>1</sup>

<sup>1</sup>*School of Molecular Sciences*, <sup>2</sup>*School of Biological Sciences*,

<sup>3</sup>*ARC Centre of Excellence in Plant Energy Biology*

*The University of Western Australia, 35 Stirling Highway, Crawley WA 6009, Australia*

<sup>4</sup>*Curtin Health Innovation Research Institute, Curtin University and the Perron Institute for Neurological and Translational Science, Sarich Neuroscience Research Institute, QEII Medical Centre, Nedlands WA 6009, Australia*

---

#### **Nomenclature**

ACN	acetonitrile
AIBN	Azobisisobutyronitrile
Ar	Argon
BCA	Bicinchoninic acid
CHAPS	3-[(3-cholamidopropyl)dimethylammonio]-1-propanesulfonate
DLS	Dynamic Light Scattering
HS	Human Serum
GMA	Glycidyl Methacrylate
FA	Formic acid
FTIR	Fourier Transform Infra-Red
GMA	Glycidyl methacrylate
LCMS	Liquid Chromatography Mass Spectrometry
MEK	Methyl ethyl ketone
NP	Nanoparticle
PBS	Phosphate Buffered Saline
PEG	Polyethylene glycol
PGMA	Poly (glycidyl methacrylate)
RhB	RhodamineB
RT	Room temperature
SDS-PAGE	Sodium dodecyl sulphate polyacrylamide gel electrophoresis
TEM	Transmission Electron Microscopy
TFA	Trifluoroacetic acid
THF	Tetrahydrofuran
TRIS	Tris(hydroxymethyl)aminomethane

## **Contents**

1. Materials
  2. Methods
  3. Supporting Tables and Figures
    - a. Figure S1. FTIR spectrum acquired from PEGylated and non-PEGylated NPs.
    - b. Figure S2. Time-based protein corona analysis of PEGylated and non-PEGylated PGMA-based NPs.
    - c. Figure S3. Hydrodynamic radii measurements of NPs with and without serum incubation measured by DLS (non-logarithmic scale)
    - d. Table S1. Normalised protein band abundance data derived from ImageJ analysis of SDS-PAGE gels.
    - e. Figure S4. Graphical representation of individual protein band abundance from human serum and hard corona samples from both PEGylated and non-PEGylated NPs with statistical significance analysed with 1-way ANOVA.
    - f. Table S2. 1-way ANOVA data of protein band abundance of human serum and hard corona samples from PEGylated and non-PEGylated NPs.
  4. References
- 

### **1. Materials**

All chemicals and reagents were purchased from Sigma-Aldrich unless otherwise stated: glycidyl methacrylate (GMA); methyl ethyl ketone (MEK, Fisher Chemicals); diethyl ether; chloroform (Merck Millipore); Pluronic-F108; MilliQ water (<18 MΩcm); rhodamineB (RhB, Fluka Chemicals); *O*-(2-aminoethyl)polyethylene glycol  $M_p$  3000. For the protein corona formation study, sterile and filtered human serum was obtained commercially. cOmplete™ Mini EDTA-free Protease Inhibitor cocktail (Roche); Urea; CHAPS; Sucrose; Sequencing-grade trypsin (Promega); LCMS Grade Water; LCMS Grade Acetonitrile (ACN); LCMS Grade trifluoroacetic acid (TFA); LCMS Grade formic acid (FA); Coomassie Blue R250 (ThermoFisher Scientific); Methanol; Acetic Acid; 4-15 % 30 μL-Mini-PROTEAN Precast polyacrylamide gel (Biorad); Ammonium Bicarbonate; sodium dodecyl sulphate (SDS); glycerol; bromophenol blue; Tris-HCl; Pierce™ BCA Assay Kit (Thermo Scientific).

### **2. Methods**

#### *a. Synthesis of PGMA*

Poly(glycidyl methacrylate) (PGMA) ( $M_w$  120000) was synthesized by radical polymerization according to a published procedure.<sup>1</sup> In brief, glycidyl methacrylate (GMA) (10.0 mL, 73.3 mmol) in methyl ethyl ketone (MEK) (10 mL) was added to a Schlenk tube, and then degassed through 3 freeze/pump/thaw cycles and backfilled with argon gas. The solution was transferred to a 50 mL two-necked round-bottomed flask fitted with a gas-tight overhead stirrer, then heated to 80 °C before azobisisobutyronitrile (AIBN) (0.2 M in toluene, 292 μL, 0.584 mmol) was added via syringe. The

reaction was stirred at 80 °C under nitrogen gas for 18 h. After which, air was allowed to enter the reaction and MEK (20 mL) added to dilute the viscous liquid. The solution was cooled to room temperature and then added slowly to methanol (600 mL). The resulting precipitate was collected by filtration. The precipitate was air-dried briefly, then dissolved in tetrahydrofuran (THF) (50 mL), filtered and re-precipitated by slow addition to methanol (600mL). The product was collected by filtration and dried to afford PGMA (8.2 g, 79%) as a white solid.

*b. Synthesis of RhB-modified PGMA*

100 mg of PGMA and 25 mg of Rhodamine B (RhB) dye were added to 30 mL MEK and refluxed for 3 hours at 70 °C. The resulting PGMA-RhB solution was reduced under pressure to ~1 mL volume at 40°C. Solid PGMA-RhB was isolated in diethyl ether and allowed to dry at room temperature.

*c. Preparation of PGMA-RhB Nanoparticles*

PGMA-RhB was dissolved in 1:3 chloroform/MEK to form an organic phase. The organic phase was added drop-wise into a vigorously stirring aqueous phase consisting of a solution of Pluronic-F108 (1.25 % (w/v)). The resulting emulsion was homogenized using a probe ultrasonicator for 10 minutes at a low power setting. After removing the solvents present in the emulsion under reduced pressure, the nanoparticle suspension was centrifuged at 3000 x g for 20 minutes and the supernatant was collected and stored at room temperature until required. Nanoparticle yield by mass was calculated by weighing out freeze-dried samples of known volume of the supernatant.

*d. PEGylation of PGMA-RhB Nanoparticles*

To prepare PEGylated PGMA-RhB NPs, 1:1 mass ratio of PGMA-RhB NPs to *O*-(2-aminoethyl) polyethylene glycol  $M_p$  3000 acquired from Sigma-Aldrich, was dispersed by sonication in 10 mL volume of deionized water and heated at 70 °C for 48 hours. The resulting suspension was centrifuged at 3000 x g for 5 minutes and the supernatant consisting of PEG-PGMA-RhB NPs was stored at room temperature until required.

*e. Fourier Transform Infra-Red (FTIR) Spectrometry*

The NP variants were freeze-dried and subjected to FTIR analysis (Perkin-Elmer) between the frequency range of 4000-450  $\text{cm}^{-1}$  with a resolution of 4  $\text{cm}^{-1}$ .

*f. Dynamic Light Scattering and Zeta Potential Measurement*

NP hydrodynamic size and size distribution were determined using Dynamic Light Scattering, which also enables zeta potential measurements corresponding to the surface charge of the NPs. (DLS, Malvern Zetasizer Nano) Briefly, neat NP suspensions were diluted in MilliQ water to an appropriate concentration and subjected to DLS and zeta potential measurements. Serum-incubated NPs had an additional step of centrifugation to wash off unbound serum proteins (3 times with 1X PBS).

The resulting NP pellet was resuspended by brief sonication prior to being subjected to DLS and zeta potential measurements.

- g. Transmission Electron Microscopy*

NP samples for TEM imaging were prepared by depositing 10  $\mu$ L of diluted NP suspension on carbon-coated copper grids. All TEM images were obtained off the dried grids at 120 kV. (JEOL JEM-2100)
- h. Protein Corona Formation on Nanoparticles*

Known masses of the NP variants were resuspended in protein concentration that mimics in vivo serum conditions<sup>2</sup> (55 % human serum in 1X PBS) and incubated for 1 hour at 37 °C with agitation. Upon completion of incubation period, the NP-serum suspension was centrifuged through a 0.7M sucrose solution at 20000 x g for 20 minutes. The serum coated NP pellet was washed with 1X PBS three times by centrifuging (3X; 15 minutes; 20000 x g) to remove all unbound serum proteins. After the final wash, the pellet was resuspended by sonication in 100-150  $\mu$ L of rehydration buffer (8M urea and 2 % (w/v) CHAPS) on ice. The resulting suspension was then centrifuged at room temperature at 20000 x g for 20 minutes and the supernatant containing hard corona proteins was collected for subsequent analyses.
- i. Bicinchoninic acid (BCA) Protein Quantification*

Protein solutions eluted from the NP samples and human serum were subjected to protein quantification according to the manufacturer's instructions using BSA as a standard.
- j. 1-D Sodium Dodecyl Sulphate (SDS) Polyacrylamide Gel Electrophoresis*

5X SDS loading buffer (250 mM Tris-HCl pH 6.8; 10 % SDS; 30 % glycerol; 5 % 2-mercaptoethanol; 0.02 % bromophenol blue) was added to the appropriate volume of protein samples and heated for 5 minutes at 95 °C. The samples were cooled and 20  $\mu$ g of protein per sample was loaded into the wells of a precast 4-15 % polyacrylamide gel. The loaded denatured protein samples were allowed to stack by running the gel at 50 V for 15 minutes. After which the samples were subjected to gel electrophoresis separation at a constant current of 15 mA. After SDS-PAGE, the gel was washed with MilliQ water and stained with Coomassie Brilliant Blue R-250 stain for 30 minutes and then destained overnight (acetic acid: methanol: water = 1:4:5) on a rocking platform at room temperature. The gels were imaged using the Biorad ChemiDoc MP system.
- k. Protein Quantitation*

The open-source scientific image analysis package, ImageJ was used to quantify the abundance of protein bands in the gel images by means of pixel measurements (n=3). The resulting data obtained from the gels was normalized to 100 (highest intensity measured in human serum sample) to enable comparison of protein band intensities.

*l. In-Gel Protein Digestion*

Protein bands from the SDS-PAGE gel were excised on a clean surface and placed in allocated wells of a 96-well plate with V-bottom configuration. Each gel slice was washed to de-stain 3X with 100  $\mu$ L 50 % (v/v) acetonitrile (ACN) in 10mM ammonium bicarbonate solution using gentle agitation on an orbital shaker for 45 minutes. Gel slices were then dried at 50 °C for 20 minutes. 20  $\mu$ L of tryptic digestion solution (12.5  $\mu$ g mL<sup>-1</sup> in 10 mM ammonium bicarbonate solution) was added to each dried gel slice and incubated at 37 °C overnight. Peptide extraction after the digestion process was performed as previously described by Shevchenko et al<sup>3</sup>. Retrieved peptides were stored at -80 °C until required for mass spectrometry analysis.

*m. Liquid Chromatography Mass Spectrometry (LC-MS)*

The peptide extracts were analysed by mass spectrometry using an Agilent 6520 Q-TOF mass spectrometer with an HPLC Chip Cube source. The Chip consisted of a 160 nL enrichment column (Zorbax 300SB-C18 5  $\mu$ ) and a 150 mm separation column (Zorbax 300SB-C18 5  $\mu$ ) driven by Agilent Technologies 1200 series nano/capillary liquid chromatography system. Both systems were controlled by MassHunter Workstation LC/MS Data Acquisition for 6500 series Q-TOF (ver B.06.01, Build 6.01.6157, Agilent Technologies). Peptides were loaded onto the trapping column at 4  $\mu$ L min<sup>-1</sup> in 5 % (v/v) ACN and 0.1 % (v/v) formic acid (FA) with the chip switched to enrichment and using the capillary pump. The chip was then switched to separation and peptides eluted during a 15 minute gradient (5 % ACN – 35 % ACN) directly into the mass spectrometer. The mass spec was run in positive ion mode and MS scans run over a range of m/z 250-1400 and at 8 spectra s<sup>-1</sup> and MS/MS scans run over a range of m/z 70-1400 and at 4 spectra s<sup>-1</sup>. Precursor ions were selected for auto MS/MS at an absolute threshold of 500 and a relative threshold of 0.01, with max 3 precursors per cycle, and active exclusion set at 2 spectra and released after 1 min. Precursor charge-state selection and preference was set to 2+, 3+ and then >3+ and precursors selected by charge then abundance. Resulting MS/MS spectra were opened in MassHunter Workstation Qualitative Analysis (ver B.07.00, Build 7.0.7024.29, Service Pack 1, Agilent Technologies) and MS/MS compounds detected by “Find Auto MS/MS” using default settings. The resulting compounds were then exported as mzdata files.

*n. Validation of Protein Identifications*

Mzdata files from MassHunter Workstation Qualitative Analysis were searched using MASCOT (version 2.5.1 Matrix Science) software and the Human UniProt database (13/04/2016, 70236 sequences) using the decoy search option of Mascot. Enzymatic digestion with trypsin was selected, along with maximum 1 missed cleavages, peptide charges + 2 and + 3, 100 ppm precursor mass tolerance and 0.25 Da fragment mass tolerance; Carbamidomethyl (C), oxidation (M) were set as variable modifications. Protein matches were only claimed if at least one significant unique peptides

were detected per protein, resulting in MOWSE scores typically higher than 70 ( $p < 0.05$  significance level is  $\text{Score} > 36$ ).

*o. Statistical Analysis*

All statistical data presented in this study were analysed using GraphPad Prism 6.0 software package. Student's *t*-test was used in the BCA quantification of hard corona proteins to determine statistical significance of the total amount of adsorbed serum proteins between PEGylated and non-PEGylated PGMA-RhB nanoparticles. 1-way ANOVA (post hoc analysis by Tukey's multiple comparisons test) was utilised for the statistical analysis of protein abundance to determine if individual protein bands observed in human serum are able to preferentially adsorb on either PEGylated or non-PEGylated PGMA-based nanoparticles.

### 3. Supporting Figures

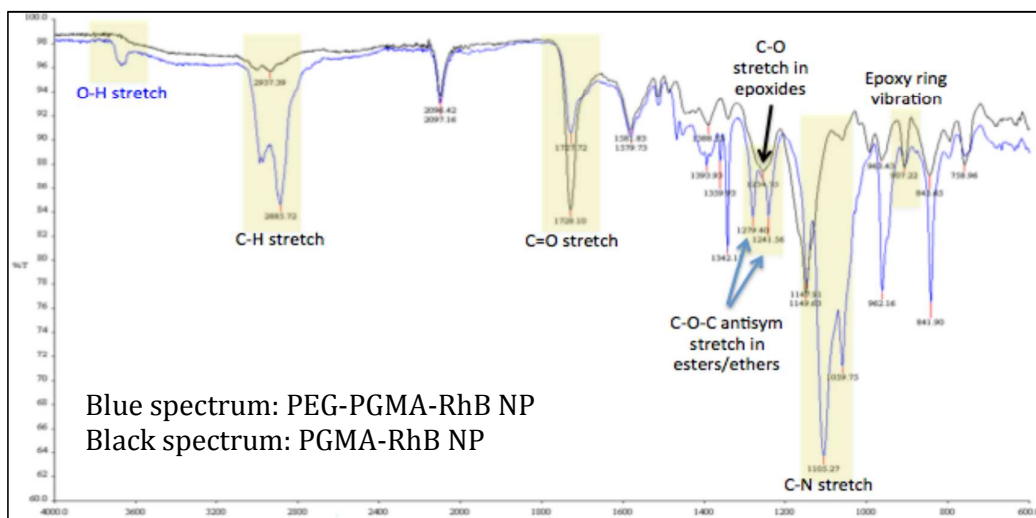


**Figure S1:** FTIR spectra indicating conjugation of PEG chains on PGMA-RhB NP surface. The epoxide rings present on the PGMA polymer backbone are highly reactive and undergo nucleophilic ring-opening reaction with O-amino (polyethylene glycol) 3000. (Refer to Figure 1A) The resulting -OH stretch at approximately  $3400\text{cm}^{-1}$  observed in the spectra is indicative of the presence of PEG chain functionalisation of the PGMA-RhB NPs.

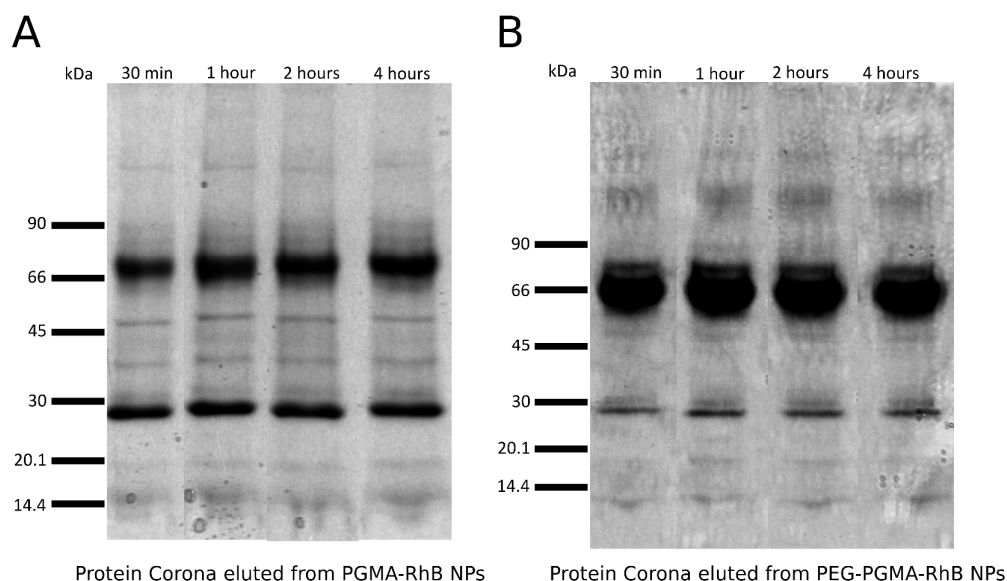


**Figure S2.** Time-based protein corona analysis from PGMA-RhB NPs (A) and PEG-PGMA-RhB NPs (B). NP samples were incubated in 55% human serum at  $37^\circ\text{C}$  from 30 minutes up to 4 hours and it was determined that the hard corona profile stabilised and remained consistent beyond 1 hour exposure to human serum. Between the 30-minute and 1-hour time points, specific protein bands in the corona indicated differences in specific protein abundances, possibly because the final hard corona composition had not been reached during that time frame.

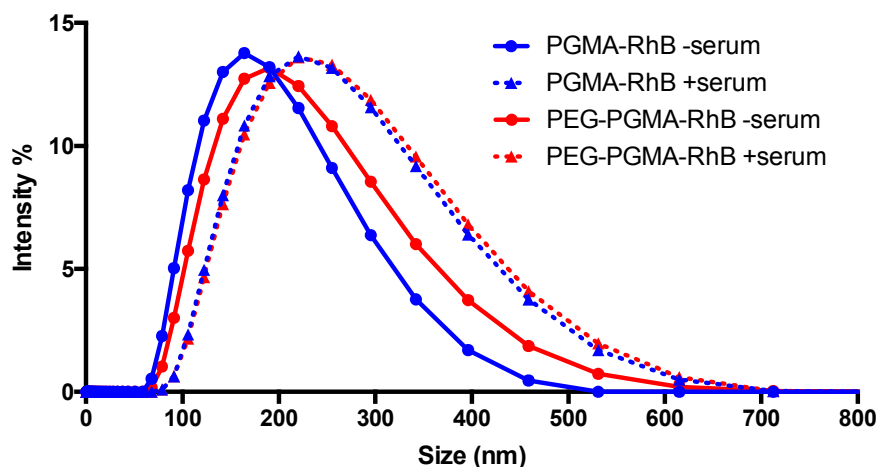
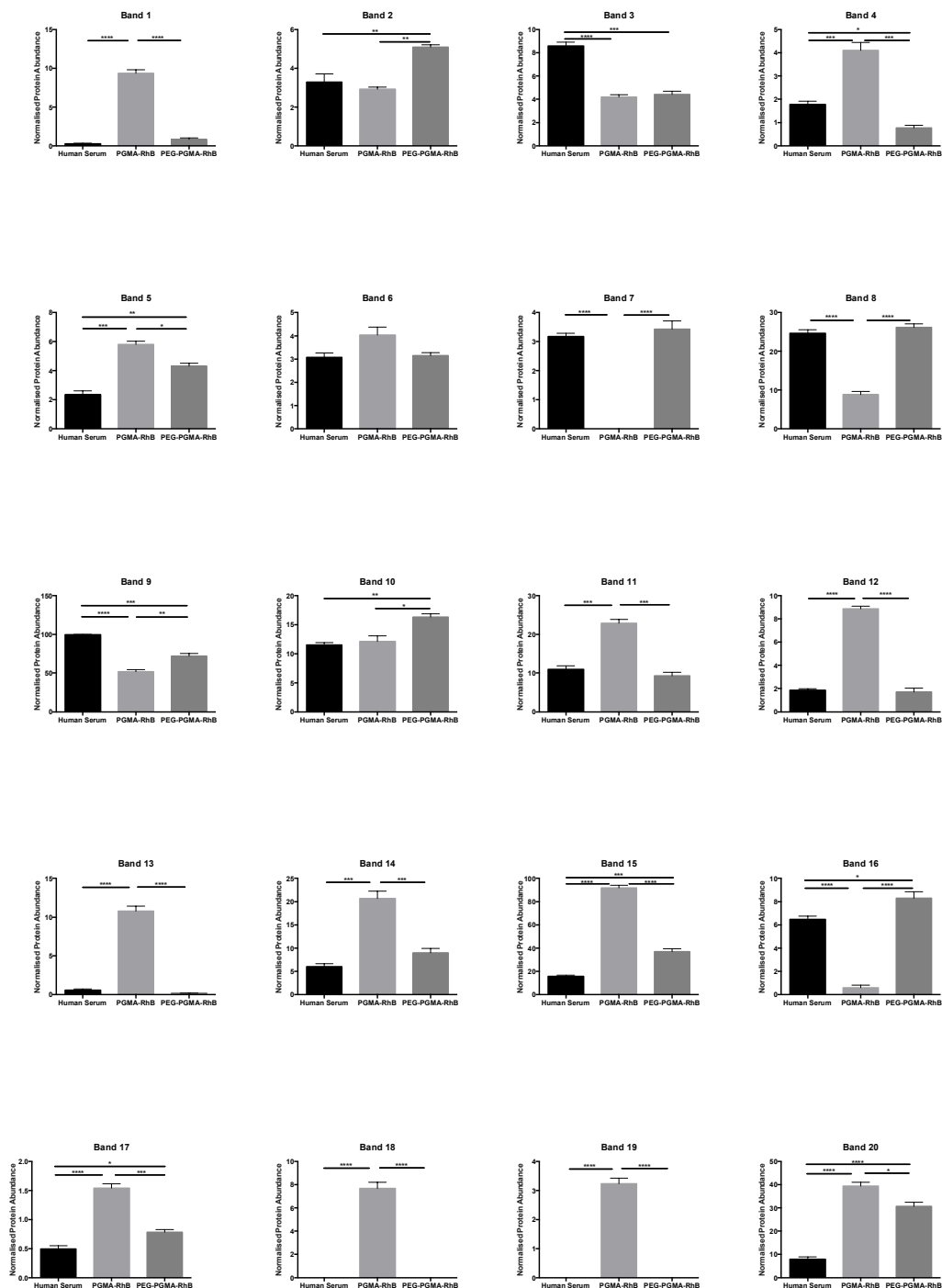


Figure S3. DLS measurements of hydrodynamic radii of NPs before and after serum incubation, represented on a non-logarithmic scale.

Table S1: Tabulation of normalised triplicate raw data of protein band abundance at observed kDa from human serum and hard corona samples from non-PEGylated and PEGylated PGMA-RhB NPs. Abundance values were derived from ImageJ analysis of the band intensities from SDS-PAGE gels and the highest value measured in human serum from each gel was normalised to 100. (n=3)

	kDa	Human Serum (1)	Human Serum (2)	Human Serum (2)	PGMA-RhB (1)	PGMA-RhB (2)	PGMA-RhB (3)	PEG-PGMA-RhB (1)	PEG-PGMA-RhB (2)	PEG-PGMA-RhB (3)
BAND 1	<200	0.18	0.25	0.40	8.66	10.28	9.01	0.73	0.54	1.23
BAND 2	180	2.48	3.57	3.84	2.85	3.15	2.76	5.09	5.29	4.89
BAND 3	160	8.63	7.94	9.14	4.01	3.99	4.57	4.31	4.93	3.98
BAND 4	140	1.51	1.81	2.01	3.86	3.68	4.78	0.63	0.69	0.99
BAND 5	120	2.79	2.40	1.84	5.87	5.38	6.17	4.23	4.69	4.00
BAND 6	100	3.03	2.77	3.43	3.81	3.81	4.69	3.03	2.99	3.42
BAND 7	90	3.35	3.20	2.99	0.00	0.00	0.00	3.30	3.98	3.00
BAND 8	75	24.25	23.19	26.42	8.14	8.00	10.44	24.55	25.94	27.88
BAND 9	66	100.00	99.54	99.74	46.73	53.21	55.73	67.97	68.96	78.93
BAND 10	54	10.73	11.72	12.05	11.48	10.95	13.98	15.53	15.95	17.43
BAND 11	47	10.00	10.08	12.74	21.73	22.10	24.83	8.01	9.02	10.93
BAND 12	45	1.58	1.95	2.01	8.40	8.91	9.25	1.36	1.50	2.32
BAND 13	40	0.38	0.88	0.43	9.64	11.85	10.91	0.19	0.20	0.19
BAND 14	35	5.18	7.34	5.52	19.12	23.84	19.03	10.84	8.19	7.98
BAND 15	30	14.07	15.00	17.84	90.47	95.92	89.46	32.55	40.93	37.83
BAND 16	20	6.35	6.06	7.00	0.96	0.24	0.60	7.53	7.94	9.37
BAND 17	18	0.50	0.39	0.59	1.42	1.67	1.54	0.86	0.69	0.80
BAND 18	15	0.00	0.00	0.00	7.01	7.30	8.73	0.00	0.00	0.00
BAND 19	13	0.00	0.00	0.00	3.14	3.59	2.98	0.00	0.00	0.00
BAND 20	11	7.50	9.84	6.53	42.75	37.30	38.16	28.09	29.93	33.93



**Figure S4: Graphical representation of individual band intensity from human serum and hard corona samples from PEGylated and non-PEGylated PGMA-based nanoparticles at designated kDa measured by ImageJ analysis. Table 2 in the manuscript summarizes the statistical significance information for each band, and the protein/s identified therein. Statistical analysis was performed by 1-way ANOVA to determine if individual proteins in human serum could preferentially adsorb on PEGylated or non-PEGylated nanoparticles. (n=3, \*p<0.05, \*\*p<0.005, \*\*\*p<0.0005 and \*\*\*\*p<0.00005)**

**Table S2: Statistical data derived using one-way ANOVA (post hoc analysis: Tukey's multiple comparisons test) to analyse individual protein band abundance from both hard corona samples compared to each other and to the respective band from human serum, \*p<0.05, \*\*p<0.005, \*\*\*p<0.0005 and \*\*\*\*p<0.00005, ns is not significantly different**

Number of families		1				
Number of comparisons per family		3				
Alpha		0.05				
	Tukey's multiple comparisons test	Mean Diff.	95% CI of diff.	Outcome	Significance	
<b>Band 1</b>	Human Serum vs. PGMA-RhB	-9.041	-10.39 to -7.692	Yes	****	
	Human Serum vs. PEG-PGMA-RhB	-0.559	-1.908 to 0.7902	No	ns	
	PGMA-RhB vs. PEG-PGMA-RhB	8.482	7.133 to 9.832	Yes	****	
<b>Band 2</b>	Human Serum vs. PGMA-RhB	0.376	-0.7463 to 1.498	No	ns	
	Human Serum vs. PEG-PGMA-RhB	-1.795	-2.917 to -0.6727	Yes	**	
	PGMA-RhB vs. PEG-PGMA-RhB	-2.171	-3.293 to -1.049	Yes	**	
<b>Band 3</b>	Human Serum vs. PGMA-RhB	4.381	3.171 to 5.591	Yes	****	
	Human Serum vs. PEG-PGMA-RhB	4.163	2.953 to 5.373	Yes	***	
	PGMA-RhB vs. PEG-PGMA-RhB	-0.2187	-1.429 to 0.9915	No	ns	
<b>Band 4</b>	Human Serum vs. PGMA-RhB	-2.33	-3.300 to -1.359	Yes	***	
	Human Serum vs. PEG-PGMA-RhB	1.008	0.03744 to 1.978	Yes	*	
	PGMA-RhB vs. PEG-PGMA-RhB	3.337	2.367 to 4.308	Yes	***	
<b>Band 5</b>	Human Serum vs. PGMA-RhB	-3.466	-4.497 to -2.435	Yes	***	
	Human Serum vs. PEG-PGMA-RhB	-1.967	-2.997 to -0.9361	Yes	**	
	PGMA-RhB vs. PEG-PGMA-RhB	1.499	0.4687 to 2.530	Yes	*	
<b>Band 6</b>	Human Serum vs. PGMA-RhB	-0.9613	-1.980 to 0.05782	No	ns	
	Human Serum vs. PEG-PGMA-RhB	-0.07133	-1.090 to 0.9478	No	ns	
	PGMA-RhB vs. PEG-PGMA-RhB	0.89	-0.1292 to 1.909	No	ns	
<b>Band 7</b>	Human Serum vs. PGMA-RhB	3.178	2.409 to 3.947	Yes	****	
	Human Serum vs. PEG-PGMA-RhB	-0.248	-1.017 to 0.5212	No	ns	
	PGMA-RhB vs. PEG-PGMA-RhB	-3.426	-4.195 to -2.657	Yes	****	
<b>Band 8</b>	Human Serum vs. PGMA-RhB	15.76	11.83 to 19.69	Yes	****	
	Human Serum vs. PEG-PGMA-RhB	-1.503	-5.431 to 2.424	No	ns	
	PGMA-RhB vs. PEG-PGMA-RhB	-17.27	-21.19 to -13.34	Yes	****	
<b>Band 9</b>	Human Serum vs. PGMA-RhB	47.87	36.83 to 58.92	Yes	****	
	Human Serum vs. PEG-PGMA-RhB	27.81	16.76 to 38.85	Yes	***	
	PGMA-RhB vs. PEG-PGMA-RhB	-20.07	-31.11 to -9.021	Yes	**	
<b>Band 10</b>	Human Serum vs. PGMA-RhB	-0.632	-3.560 to 2.296	No	ns	
	Human Serum vs. PEG-PGMA-RhB	-4.801	-7.729 to -1.872	Yes	**	
	PGMA-RhB vs. PEG-PGMA-RhB	-4.169	-7.097 to -1.240	Yes	*	
<b>Band 11</b>	Human Serum vs. PGMA-RhB	-11.95	-15.90 to -7.994	Yes	***	
	Human Serum vs. PEG-PGMA-RhB	1.616	-2.339 to 5.571	No	ns	
	PGMA-RhB vs. PEG-PGMA-RhB	13.57	9.610 to 17.52	Yes	***	
<b>Band 12</b>	Human Serum vs. PGMA-RhB	-7.006	-8.032 to -5.979	Yes	****	
	Human Serum vs. PEG-PGMA-RhB	0.116	-0.9108 to 1.143	No	ns	
	PGMA-RhB vs. PEG-PGMA-RhB	7.122	6.095 to 8.148	Yes	****	
<b>Band 13</b>	Human Serum vs. PGMA-RhB	-10.24	-11.89 to -8.590	Yes	****	
	Human Serum vs. PEG-PGMA-RhB	0.3677	-1.280 to 2.015	No	ns	
	PGMA-RhB vs. PEG-PGMA-RhB	10.61	8.958 to 12.25	Yes	****	
<b>Band 14</b>	Human Serum vs. PGMA-RhB	-14.65	-19.54 to -9.757	Yes	***	
	Human Serum vs. PEG-PGMA-RhB	-2.99	-7.881 to 1.901	No	ns	
	PGMA-RhB vs. PEG-PGMA-RhB	11.66	6.767 to 16.55	Yes	***	
<b>Band 15</b>	Human Serum vs. PGMA-RhB	-76.32	-84.73 to -67.90	Yes	****	
	Human Serum vs. PEG-PGMA-RhB	-21.46	-29.88 to -13.04	Yes	***	
	PGMA-RhB vs. PEG-PGMA-RhB	54.85	46.43 to 63.27	Yes	****	
<b>Band 16</b>	Human Serum vs. PGMA-RhB	5.873	4.227 to 7.518	Yes	****	
	Human Serum vs. PEG-PGMA-RhB	-1.813	-3.458 to -0.1670	Yes	*	
	PGMA-RhB vs. PEG-PGMA-RhB	-7.685	-9.331 to -6.040	Yes	****	
<b>Band 17</b>	Human Serum vs. PGMA-RhB	-1.051	-1.313 to -0.7892	Yes	****	
	Human Serum vs. PEG-PGMA-RhB	-0.289	-0.5511 to -0.02692	Yes	*	
	PGMA-RhB vs. PEG-PGMA-RhB	0.7623	0.5002 to 1.024	Yes	***	
<b>Band 18</b>	Human Serum vs. PGMA-RhB	-7.675	-9.007 to -6.344	Yes	****	
	Human Serum vs. PEG-PGMA-RhB	0	-1.331 to 1.331	No	ns	
	PGMA-RhB vs. PEG-PGMA-RhB	7.675	6.344 to 9.007	Yes	****	
<b>Band 19</b>	Human Serum vs. PGMA-RhB	-3.237	-3.699 to -2.774	Yes	****	
	Human Serum vs. PEG-PGMA-RhB	0	-0.4624 to 0.4624	No	ns	
	PGMA-RhB vs. PEG-PGMA-RhB	3.237	2.774 to 3.699	Yes	****	
<b>Band 20</b>	Human Serum vs. PGMA-RhB	-31.45	-37.97 to -24.92	Yes	****	
	Human Serum vs. PEG-PGMA-RhB	-22.69	-29.22 to -16.17	Yes	****	
	PGMA-RhB vs. PEG-PGMA-RhB	8.752	2.226 to 15.28	Yes	*	

## References

1. V. Tsyalkovsky, V. Klep, K. Ramaratnam, R. Lupitsky, S. Minko and I. Luzinov, *Chemistry of Materials*, 2008, **20**, 317-325.
2. A. Jedlovsky-Hajdú, F. B. Bombelli, M. P. Monopoli, E. Tombácz and K. A. Dawson, *Langmuir*, 2012, **28**, 14983-14991.
3. A. Shevchenko, H. Tomas, J. Havlis, J. V. Olsen and M. Mann, *Nat. Protocols*, 2007, **1**, 2856-2860.